Evolution of Microstructure and Properties in Alpha-Brass after Iterative Processing

VALERIE RANDLE and HELEN DAVIES

Iterative strain-recrystallization cycles have been applied to alpha-brass in order to enhance ductility while maintaining tensile strength. Five iterations of 25 pct uniaxial strain followed by a 300 second anneal at 665 °C were used to achieve the desired properties. This article concentrates on assessment of the effect of the processing on microstructure evolution and crystallographic details of the grain boundary population, after *each* strain-recrystallization cycle. The overall aim of the work is to provide further knowledge on the mechanisms of grain boundary engineering. The results demonstrate that there is a distinctive pattern in both the $\Sigma 3$ population density (in coincidence site lattice notation) and the proximity to the Σ reference structure, as a function of treatment cycle iteration. During the first two treatment cycles, the proportion of $\Sigma 3$s drops, which the present work shows is an essential step to homogenize the microstructure in preparation for the subsequent treatment iterations required for the property enhancements to develop. It is proposed that this is a general feature of all grain boundary engineering by iterative processing where cold reduction is involved. Furthermore, $\Sigma 3^n$ ($n > 1$) boundaries do not build up in the microstructure concomitant with the $\Sigma 3$ fraction because they are removed by the "$\Sigma 3$ regeneration model."

I. INTRODUCTION

IT is now known that various types of intergranular phenomena are linked to grain boundary structure, and if the crystallography of these boundaries can be controlled, certain material properties can be improved. This has come to be known as "grain boundary engineering." For example, grain boundary engineering has been known to mitigate intergranular stress corrosion cracking in nickel-based alloys[1] and to influence mechanical behavior such as ductility.[2,3]

Successful manipulation of grain boundary structure in nickel-based face-centered cubic (fcc) metals and alloys has been achieved by iterative thermomechanical processing. The steps are (1) cold work to a level less than the total reduction required; (2) annealing at a temperature above the recrystallization temperature and usually a time short enough to limit grain growth; and (3) repetition of steps (1) and (2) until the total forming reduction has been achieved and the profile of grain boundary structure has been sufficiently changed, with accompanying modification to selected properties.[4] Some procedures alternatively employ strain-anneal cycles rather than strain-recrystallization cycles. In general, strain-anneal cycles result in larger grain sizes.[3,5]

The grain boundary population has customarily been characterized by the proportion of low-Σ coincidence site lattice (CSL) boundaries in the sample, where Σ is the reciprocal density of coinciding sites. A subset of the $\Sigma 3$ CSL class is the annealing twin. In those fcc metals and alloys that readily form annealing twins, the grain boundary population is therefore often dominated by $\Sigma 3$ and $\Sigma 3^n$. The $\Sigma 3$s are the only CSL class with $\Sigma > 1$ known, in bulk three-dimensional polycrystals, *consistently* to exhibit "special" (*i.e.*, better than average) properties.

In the present article, we investigate the application of grain boundary engineering principles, *i.e.*, iterative strain-recrystallization cycles, to grain boundaries in alpha-brass in order to achieve enhanced ductility while maintaining tensile strength. There are three objectives: to assess the effect after *each* strain-recrystallization cycle on microstructure evolution and crystallographic details of the grain boundary population; to measure the effect of these changes on strain to failure; and to gain further knowledge of the mechanisms of grain boundary engineering, which are as yet incompletely understood. Most investigations that employ iterative treatments to enhance properties do not report the interim effects on microstructure, only the final effect. It is anticipated that study of the intermediate steps will provide clues to the mechanisms that control the process.

II. EXPERIMENTAL DETAILS

Ten flat tensile specimens of alpha-brass (melting point 900 °C) with gage length 40 mm and 6×1 mm^2 cross section were strained 25 pct, followed by an air anneal at 665 °C ($0.8T_m$) for 300 seconds. These parameters were scaled from other grain boundary engineering works on austenitic steels.[4] One specimen was metallographically prepared so that the grain size, microhardness, and grain boundary parameters (using electron backscatter diffraction (EBSD) in a scanning electron microscope (SEM)) could be obtained.[6] A second specimen was tensile tested to failure at room temperature on a 50 KN Hounsfield Tensometer at a rate of 5 mm/min. Load and specimen extension measurements were recorded using in-house software to construct stress/strain curves.

The remaining eight tensile specimens underwent a second iteration of the thermomechanical treatment described previously (25 pct strain, anneal 300 seconds at 665 °C).

VALERIE RANDLE, Professor, is with the Department of Materials Engineering, University of Wales, Swansea SA2 8PP, United Kingdom. Contact e-mail v.randle@swansea.ac.uk HELEN DAVIES, Process Technologist, is with INCO Europe Ltd., Clydach, Swansea, UK. Contact e-mail hmdavies@inco.com

Manuscript submitted October 2, 2001.

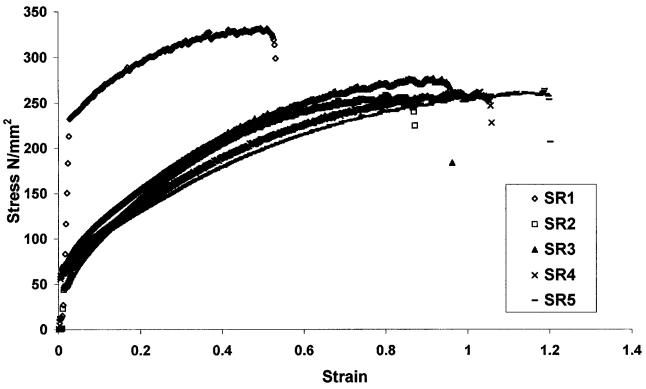

Fig. 1—Stress-strain curves after tensile testing to failure for each of the five strain-recrystallization specimens.

Again, grain size, microhardness, and grain boundary parameter measurements were obtained from one specimen and another was tensile tested to failure. The procedure was repeated on the remaining specimens until they were used up, making five iterations in all, SR1 through SR5.

Metallographic specimen preparation included a final polish using silica slurry and etching in ferric chloride solution to ensure a suitable finish for EBSD. An Oxford Instruments (High Wycombe, U.K.) OPAL EBSD system interfaced to a JEOL* 6100 SEM was used for the grain boundary misorientation analysis. Several orientation maps were obtained from each specimen. Proportions of CSL boundaries were outputted directly from the OPAL software, and in-house programs were used to compute the proximity to the exact reference misorientation.

*JEOL is a trademark of Japan Electron Optics Ltd., Tokyo.

III. RESULTS

The average Vickers hardness after application of the first 25 pct strain increment was 148 Hv; after each annealing cycle of 5 minutes at 665 °C, the average Vickers hardness dropped to 70 to 80Hv. This large reduction in hardness indicated that 5 minutes anneal at 665 °C was sufficient for recrystallization to have initiated during each iterative cold work/anneal cycle. The total cold reduction equivalent to the five iterative steps is given by

$$(1 - r_t) = (1 - r_i)^n$$

where n is the number of iterations, r_i is the cold reduction per iteration, and r_t is the equivalent total reduction.[4] From this formula, r_t is 76 pct. Figure 1 shows the stress-strain curves for each specimen. After the first treatment stage, SR1, the tensile strength is 310 N mm^{-2} and the strain to failure is 0.53. Full ductility has not yet been achieved. In stages SR2, SR3, SR4, and SR5, the tensile strength has dropped to a constant value of approximately 220 N mm^{-2}, yet the strain to failure has increased with each iteration from 0.87 to 1.20. These ductility increments are, in part, due to the increase in grain size from 20 to 52 μm, although it is unlikely to account entirely for an increase in strain to failure from 0.53 to 1.20, with no accompanying reduction in tensile strength.

The crystallographic parameters measured after each iteration were the proportion of $\Sigma 3^n (n < 4)$ and the normalized

Table I. Summary of the Main Parameters Measured for Each Specimen

Specimen	Pct $\Sigma 3$	Pct $\Sigma 9 + 27$	Grain Size (μm)	v/v_m (Mode)	Strain to Failure
SR1	23	4	20	0.35	0.53
SR2	19	2	26	0.55	0.87
SR3	26	6	47	0.45	0.96
SR4	30	3	51	0.45	1.06
SR5	34	8	54	0.25	1.20

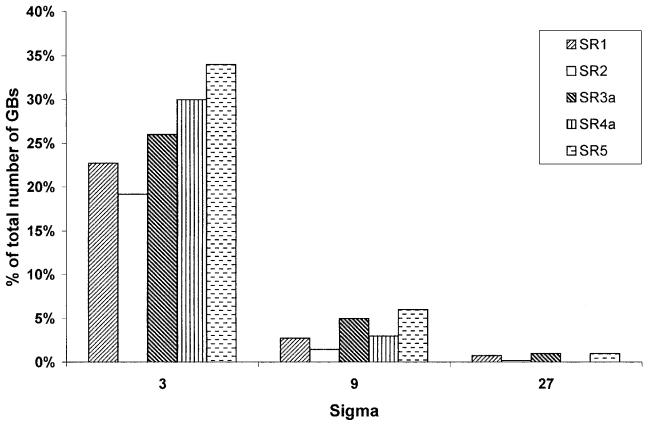

Fig. 2—Proportions (as a number percentage of total boundaries) of $\Sigma 3$, $\Sigma 9$, and $\Sigma 27$ boundaries in each of the five strain-recrystallization specimens.

proximity to the exact Σ reference structure, denoted v/v_m, where v is the actual deviation from the reference structure and v_m is the maximum allowable deviation according to the Brandon criterion, *i.e.*, 8.7 deg for $\Sigma 3$.[7] The key data are summarized in Table I for each of the five iterations. Figure 2 shows the proportions of $\Sigma 3^n$ boundaries after each iteration. No other CSL boundaries with values above that for random generation were recorded in the sample populations.

There is a considerable difference in $\Sigma 3$ proportions for each specimen. Initially, the total $\Sigma 3$ proportions are quite low (SR1, 23 pct), and there is a further reduction after the second iteration (SR2, 19 pct). Thereafter, the $\Sigma 3$ proportions increase steadily with each iteration (SR3, 26 pct; SR4, 30 pct; and SR5, 34 pct). By comparison, prior to any treatments, the $\Sigma 3$ proportion in the starting microstructure was 50 pct. The absolute $\Sigma 3$ numbers after the treatments appear to be rather low (23 to 34 pct of all boundaries) compared to examples from previous work (*e.g.*, References 3 and 8). This is a consequence of the particular data processing algorithm used in the OPAL software to transform the projected area (length) fraction of Σ boundaries into a number fraction. The two methods of data collection—length and number—result in dissimilar statistics, which are not linked by any functional relationship.[9] For the case of $\Sigma 3$, the proportion has previously been observed to be reduced by about one-third for "length" data compared to "number" data acquired from maps.[10] However, the interesting feature in the present investigation is the change in relative proportions of $\Sigma 3^n$s after each treatment cycle, rather than the absolute quantity. Processing $\Sigma 3^n$ boundaries by number rather than length has advantages for capturing $\Sigma 9$ and $\Sigma 27$

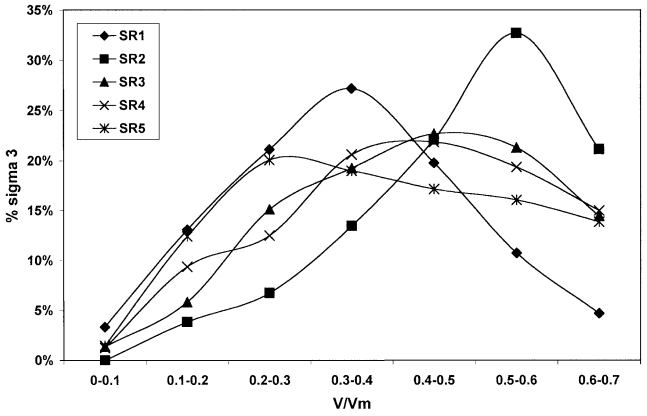

Fig. 3—Frequency distribution of v/v_m values ($\Sigma 3$ boundaries) for each of the five strain-recrystallization specimens.

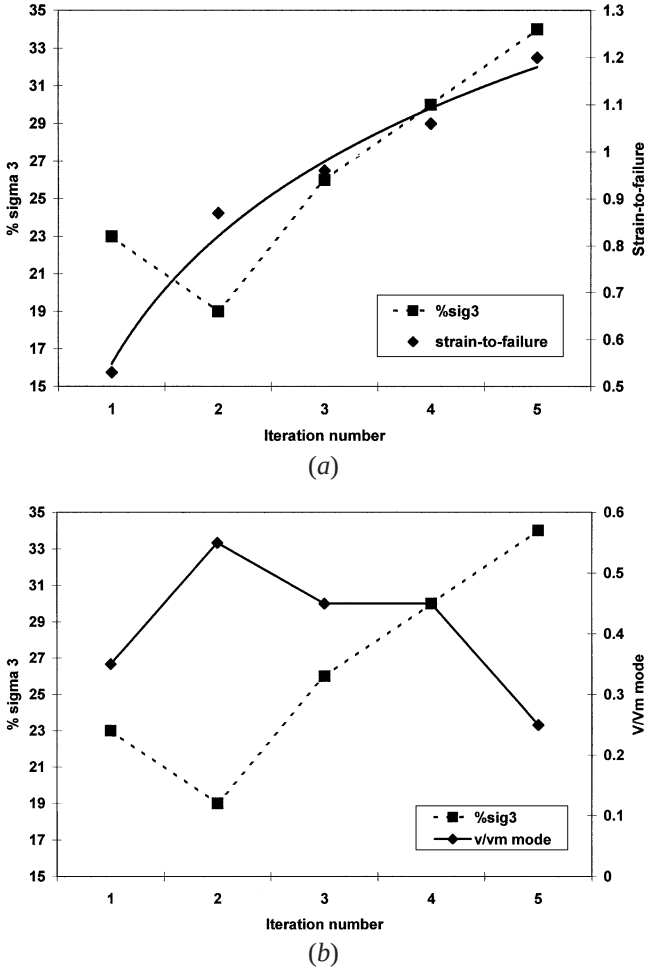

Fig. 4—(*a*) Evolution of strain to failure and proportion of $\Sigma 3$ boundaries and (*b*) inverse relationship between v/v_m and proportion of $\Sigma 3$ boundaries for each of the five strain-recrystallization specimens.

boundaries because their importance often relates to their number and location in the microstructure more than to their length. In the present data, the $\Sigma 9$ proportions are only 0.1 to 0.23 of the $\Sigma 3$ fractions. The $\Sigma 27$ proportion is insignificant (<2 pct).

The v/v_m parameter provides an indication of the proximity of each $\Sigma 3$ boundary to the reference misorientation. Hence, $v/v_m = 0$ refers to the exact CSL misorientation and $v/v_m = 1$ is the CSL limit according to the Brandon criterion. Whereas an average v/v_m could be calculated for the $\Sigma 3$s in each specimen, it is more instructive to consider the distribution profile of v/v_m values for each specimen, which is shown in Figure 3. For each specimen, there is a single maximum on the v/v_m distribution, *i.e.*, a mode value, which is included in Table I as a convenient way to characterize the distribution with a single parameter. For specimen SR1, the mode is 0.35, in the midrange for v/v_m. The distribution for SR2 is quite different, with a sharp peak at 0.55, in the upper range. Mode values of SR3 and SR4 both fall midway between the first two, with quite a flat peak at 0.45. Finally, SR5 has both the lowest mode value, 0.25, and the most diffuse profile because the distribution has a tail toward the upper end.

IV. DISCUSSION

The applied iterative treatments have clearly been successful in achieving their objective of grain boundary engineering brass specimens in order to achieve improved strain to failure for constant tensile strength. This has been accompanied by a distinct pattern in the $\Sigma 3^n$ population characteristics, as summarised on Figure 4(a). The trend was for an initial *drop* in the proportion of $\Sigma 3$s at stages SR1 and SR2 followed by a steady increase in $\Sigma 3$s throughout stages SR3, SR4, and SR5. There was an inverse correlation between $\Sigma 3$ proportions and the mode of v/v_m, as summarized on Figure 4(b).

In order to track the origins of the microstructural evolution, we will now examine each stage in detail. After the first stage, SR1, the form of the stress/strain curve compared to subsequent stages SR2 onward indicates that strain was still retained in the lattice. This is because, although it is well known that random high-angle grain boundaries act as sinks for dislocations during recrystallization, boundaries that have a periodic structure, such as $\Sigma 3$s, have a reduced dislocation annihilation rate during annealing compared to random boundaries. Hence, extrinsic dislocations tend to become pinned in pre-existing dislocation arrays in periodic boundaries.[11] Furthermore, a high proportion of twins present before the start of the iterative processing has been previously observed to increase the internal stress by creating a back stress as dislocations pile up at the immobile twins.[5] At the end of stage SR1, the proportion of $\Sigma 3$s had reduced drastically from 50 to 23 pct, indicating that the mobile boundaries—the random fraction, most able to absorb dislocations—had moved through the microstructure and destroyed many of the twins, also relieving some of the back stress caused by the retained dislocations. There is no evidence that generation of new twins had taken place during this grain boundary migration.

During SR1, the effect of dislocation pileup at pre-existing twins meant that there was insufficient annealing time to remove all the effects of the applied strain, so the second increment of 25 pct strain at the start of SR2 had an additive effect, resulting in a higher driving force for recrystallization during the annealing cycle of SR2 than during SR1. At the end of stage SR2, the proportion of $\Sigma 3$s had dropped further and, significantly, the v/v_m profile has moved to higher values, which means that the structure of such $\Sigma 3$s with

high v/v_m is similar to that of random boundaries. The higher v/v_m values can be attributed to trapped extrinsic dislocations. The upshot is that because random-type boundaries dominate the boundary population, and there are relatively few pre-existing twins to create obstructions, dislocation absorption during recrystallization can now proceed unhindered and the ductility increases proportionately. As in SR1, few new twins are generated, because v/v_m is predominantly high.

From stage SR3 onward, the desired outcome of increased ductility for constant strength begins to develop. With the SR3 increment of strain, the $\Sigma 3$ proportion begins to recover, the grain size increases, and the v/v_m profile shifts to smaller mode values. Now, with few pre-existing twins to retain strain in the system, the action of the new strain increment at the start of SR3 *acts directly on the grain boundaries*, giving rise to four possible cases when dislocations are absorbed in moving boundaries:

(1) migration of random boundaries without new twinning;
(2) migration of random boundaries with new twinning;
(3) migration of mobile $\Sigma 3$s, *i.e.*, those with medium/high v/v_m; and
(4) interaction of $\Sigma 3$s from (2) and (3).

Whereas it is not possible from the data to know the relative contributions of (1) through (4), there is experimental evidence that they are all operating to some extent. The evidence for (1) is that the grain size increases; the evidence for (2) is that a minor proportion of $\Sigma 3$s have low v/v_m, which means they are probably new twins. Case (3) is implied by the increase in $\Sigma 3$ fraction, accompanied by medium-to-high v/v_m plus a slight increase in $\Sigma 9$. Multiplication of $\Sigma 3$s and $\Sigma 3^n$s by impingement implies that there is a *critical threshold density*, which has now been exceeded and interactions of the type $\Sigma 3 + \Sigma 3 = \Sigma 9$ are taking place. However, the aggregated proportion of $\Sigma 3^n$ ($n > 1$) does not build up in the microstructure through stages SR3 to SR5 because they, $\Sigma 9$ and $\Sigma 27$, are removed by the "$\Sigma 3$ regeneration model."[12] In brief, The $\Sigma 3$ regeneration model states that where $\Sigma 3^n$ interactions take place, $\Sigma 3^{n+} + \Sigma 3^n \rightarrow \Sigma 3$ is the favorable outcome rather than $\Sigma 3^{n+1} + \Sigma 3^n \rightarrow \Sigma 3^{n+2}$, and in this way, mobile $\Sigma 3$s, as distinct from new twins, are replenished in the microstructure.

The features established during SR3 of an increase in $\Sigma 3$ proportion accompanied by an increase in ductility continue throughout SR4 and SR5. However, at the end of SR5, a v/v_m profile, which is now considerably displaced to lower values and has the lowest mode value of all the iterations, is recorded. This means either that the rate of new twin generation has increased, or there is "fine tuning" toward the lowest energy positions of $\Sigma 3$s already present,[8] or a combination of both.

Looking at the microstructure evolution as a whole, the change point comes during SR3. The main difference between the staring specimen and SR3 is that for the latter case the microstructure has effectively been *primed* for subsequent $\Sigma 3$ generation and interactions, which lead to the multiplication of desirable boundaries, by the processes occurring during SR1 and SR2. These results establish that SR1 and SR2 are essential preliminary stages in the overall grain boundary engineering even though on their own they do not achieve the end product. In previous work, where grain boundary engineering was employed to enhance corrosion resistance at grain boundaries, high proportions of low v/v_m $\Sigma 3$s constituted the optimal microstructure. The present work, although not specifically addressing intergranular corrosion, indicates that several treatment iterations are required to achieve a "fine tuned" microstructure, enhanced by low v/v_m $\Sigma 3$s.

It is significant to note that the trend in $\Sigma 3$ proportions, v/v_m, and increased ductility with retained strength observed here has exactly the same features—*i.e.*, initial drop in $\Sigma 3$s, *etc*—as that found after a matrix of strain-annealing (rather than recrystallization) experiments on brass. A different time/temperature schedule was used to that employed here, namely, iterations of 15 pct strain followed by 15 minutes anneal at 600 °C ($0.73T_m$).[13] A slightly lower final ductility was achieved *via* strain annealing, 0.93, but only four iterations were applied, not five. Moreover, as noted in Section I, the majority of investigations on iterative grain boundary engineering treatments do not report individually the interim stages. However, one report on grain boundary optimization in pure copper describes in detail low strain (6 pct), two-stage treatments.[14] It is interesting to note that during the first stage the proportion of $\Sigma 3$s *dropped* compared to the starting material and increased dramatically during the second (final) stage. Furthermore, the deviation from exact $\Sigma 3$ misorientation (termed v/v_m here) increased to accompany the drop in $\Sigma 3$ and decreased with the increase in $\Sigma 3$ in the second stage. These features are totally consistent with, and support, those observed in the present work.

The finding both from the present work and comparison with other investigations is that several treatment iterations are required to optimize a grain boundary population because the initial stages are essential homogenization steps. These homogenization steps involve reduction of $\Sigma 3$ boundaries. Finally, there is no single, unique grain boundary engineering prescription of thermomechanical processing for a particular material; comparison of the present strain-recrystallization iterations compared with previous strain annealing iterations in the same material[13] suggest that there is a multiplicity of strain/time/temperature profiles, whose effect will be influenced by the starting microstructure, which can combine to bring about the desired improvement in properties.

V. CONCLUSIONS

1. Custom-designed, iterative strain-recrystallization treatments have increased ductility while maintaining constant tensile strength in alpha brass.
2. There is a distinctive pattern in both the $\Sigma 3$ population density and the proximity to the reference structure as a function of treatment cycle iteration. During the first two treatment cycles, the proportion of $\Sigma 3$s drops, which is an essential step in order to homogenize the microstructure in preparation for the subsequent treatment iterations during which the required property enhancements develop. It is suggested that this is a general mechanism for all grain boundary engineering by iterative processing where cold reduction is involved.
3. $\Sigma 3^n$ ($n > 1$) boundaries do not build up in the microstructure concomitant with the $\Sigma 3$ fraction because they are removed by the "$\Sigma 3$ regeneration model."

REFERENCES

1. B. Alexandreanu, B. Capell, and G.S. Was: *Mater. Sci. & Eng.* 2001, vol. A300, pp. 94-104.
2. E.M. Lehockey, G. Palumbo, K.T. Aust, U. Erb, and P. Lin: *Scripta Mater.*, 1998, vol. 39 (3), pp. 341-46.
3. H.M. Davies and V. Randle: *Phil. Mag.*, 2001, vol. 81A, pp. 2553-64.
4. G. Palumbo: International Patent No. WO 94/14986, 1994.
5. V. Thaveeprungsriporn and G.S. Was: *Metall. Mater. Trans. A.* 1997, vol. 28A, pp. 2101-12.
6. V. Randle and O. Engler: *Introduction to Texture Analysis: Macrotexture, Microtexture and Orientation Mapping*, Gordon and Breach Science Publishers, Holland, 2000.
7. D.G. Brandon: *Acta Metall.*, 1966, vol. 14, pp. 1479-84.
8. C.T. Thomson and V. Randle: *Acta Mater.*, 1997, vol. 45, pp. 4909-16.
9. J. Bystrzycki, R.A. Varin, M. Nowell, and K.J. Kurzydlowski: *Intermetallics*, 2000, vol. 8, pp. 1049-59.
10. W.E. King, J.S. Stolken, M. Kumar, and A.J. Schwartz: in *Electron Backscatter Diffraction in Materials Science*, A.J. Schwartz, M. Kumar, and B.L. Adams, eds., Kluwer Academic, New York, NY, 2000, pp. 153-70.
11. A.H. King: *Scripta Metall.*, 1985 vol. 19, pp. 1517-20.
12. V. Randle: *Acta Mater.*, 1999, vol. 47, pp. 4187-96.
13. H.M. Davies and V. Randle: *Mater. Sci. Technol.*, 2000, vol. 16, pp. 1399-1402.
14. W.E. King and A.J. Schwartz: *Scripta Mater.*, 1998, vol. 38 (3), pp. 449-55.